



Aalborg Universitet

AALBORG UNIVERSITY  
DENMARK

## A Numerical Matrix-Based Method for Stability and Power Quality Studies Based on Harmonic Transfer Functions

Dowlatabadi, Mohammadkazem Bakhshizadeh; Blaabjerg, Frede; Hjerrild, Jesper; Wang, Xiongfei; Kocewiak, ukasz Hubert; Bak, Claus Leth

*Published in:*

I E E E Journal of Emerging and Selected Topics in Power Electronics

*DOI (link to publication from Publisher):*

[10.1109/JESTPE.2017.2742241](https://doi.org/10.1109/JESTPE.2017.2742241)

*Publication date:*

2017

*Document Version*

Accepted author manuscript, peer reviewed version

[Link to publication from Aalborg University](#)

*Citation for published version (APA):*

Dowlatabadi, M. B., Blaabjerg, F., Hjerrild, J., Wang, X., Kocewiak, . H., & Bak, C. L. (2017). A Numerical Matrix-Based Method for Stability and Power Quality Studies Based on Harmonic Transfer Functions. *I E E E Journal of Emerging and Selected Topics in Power Electronics*, 5(4), 1542 - 1552.  
<https://doi.org/10.1109/JESTPE.2017.2742241>

### General rights

Copyright and moral rights for the publications made accessible in the public portal are retained by the authors and/or other copyright owners and it is a condition of accessing publications that users recognise and abide by the legal requirements associated with these rights.

- ? Users may download and print one copy of any publication from the public portal for the purpose of private study or research.
- ? You may not further distribute the material or use it for any profit-making activity or commercial gain
- ? You may freely distribute the URL identifying the publication in the public portal ?

### Take down policy

If you believe that this document breaches copyright please contact us at [vbn@aub.aau.dk](mailto:vbn@aub.aau.dk) providing details, and we will remove access to the work immediately and investigate your claim.

# A Numerical Matrix-Based Method for Stability and Power Quality Studies Based on Harmonic Transfer Functions

Mohammad Kazem Bakhshizadeh, *Student Member, IEEE*, Frede Blaabjerg, *Fellow, IEEE*, Jesper Hjerrild, Xiongfei Wang, *Senior Member, IEEE*, Łukasz Kocewiak, *Senior Member, IEEE*, and Claus Leth Bak, *Senior Member, IEEE*

**Abstract**— Some couplings exist between the positive- and negative-sequence impedances of a voltage sourced power converter especially in the low frequency range due to the nonlinearities and low bandwidth control loops like the PLL. In this paper, a new numerical method based on the Harmonic Transfer Function for analysis of the Linear Time Periodic systems is presented, which is able to handle these couplings. In a balanced three-phase system, there is only one coupling term, but in an unbalanced (asymmetrical) system, there are more couplings, and therefore, in order to study the interactions between these couplings a matrix based method should be used. No information about the structure of the converter is needed and elements are modelled as black boxes with known terminal characteristics. The proposed method is applicable for both power quality (harmonic and inter-harmonic emissions) and stability studies, which is verified by simulations in this paper.

**Index Terms**— Asymmetry; Black box modelling; Current control; Frequency coupling; Power converter; Unbalanced systems.

## I. INTRODUCTION

HARMONIC emission from power electronic components in modern wind farms is inevitable [1]–[3]. Even though the power electronic converters offer more efficiency and controllability, they may trigger the parallel and series resonances in the power system [4]. They may also interact with each other or with passive network elements, leading to instability [5], [6]. Hence, stable operation of wind farms with an acceptable harmonic emission level must be verified for different situations in the design phase.

The effects of the outer control loops such as the synchronization and power control loop cannot be neglected in the low frequency range (i.e. around the fundamental frequency). It has been found that the Phase-Locked Loop

(PLL) may introduce a negative damping with a frequency coupling between the input voltage and output current [7], [8]. This effect may further lead to instability in weak grids, where the resonances are located at lower frequencies. The situation is even worse when the grid and the high voltage grid connection system assets are unbalanced, for instance due to the asymmetrical displacement of the conductors in flat formation underground transmission cables, where more couplings between the frequency components exist, and consequently finding an analytic solution is very difficult [9], [10]. Modelling a balanced system in the dq domain solves the problems of the low frequency couplings [11], however, there exist a coupling between d- and q-channels. Also, for unbalanced networks; the couplings appear in the dq signals [12], and therefore, a matrix-based method is inevitable.

In [13] a new numerical matrix-based method has been presented that can easily consider all couplings in the impedance model of a power converter. In this method, a given converter is treated like a black-box, and no modelling and knowledge are needed for the system under study. Some frequency excitation tests are just needed for the system under study, which can be obtained from a full-detailed simulation model or from experiments. Therefore, different kinds of control strategies such as asymmetrical current control can also be studied with the same method. Another advantage is that it uses numerical data instead of very complicated analytic expressions (in case of a multi-converter system the complexity increases rapidly). Moreover, the parameters, structure and control of power converters are sometimes confidential, and therefore, the frequency response is only available as a numerical lookup table obtained from some measurements. Also for some passive elements the numerical representation is less complicated e.g. the grid impedance can be modelled as a numerical look-up table instead of a high order passive network formed of many elements [14]. In addition to all the above-mentioned reasons, finally the numerical evaluation methods such as the Nyquist plot may be used for stability assessment. Thus, using numerical data is advantageous in many cases.

In this paper, the matrix based method will be extended to unbalanced three-phase systems, which are more difficult to analyze due to a more complicated current controller and also

Manuscript received February 27, 2017; revised May 17, 2017 and July 11, 2017; accepted August 10, 2017. This work was supported in part by the DONG Energy Wind Power A/S and in part by the Innovation Fund Denmark.

M. K. Bakhshizadeh, J. Hjerrild, and Ł. Kocewiak are with the DONG Energy Wind Power, Fredericia 7000, Denmark (e-mail: mok@et.aau.dk; jeshj@dongenergy.dk; lukko@dongenergy.dk).

F. Blaabjerg, X. Wang, and C. L. Bak are with the Department of Energy Technology, Aalborg University, Aalborg DK-9220, Denmark (e-mail: fbl@et.aau.dk; xwa@et.aau.dk; clb@et.aau.dk).

existence of more frequency couplings. This paper is organized as follows, first the couplings in balanced and unbalanced power electronic based systems are introduced, then the matrix frequency response is briefly presented, and finally the proposed method is used in an unbalanced system that uses an asymmetrical current controller.

## II. FREQUENCY COUPLINGS IN A POWER CONVERTER

One way to study the stability of nonlinear control systems is to linearize the system around the operating point and to use linear methods for the small signal incremental equations. Therefore, the Impedance Based Stability Criterion (IBSC) can be applied to small signal impedances. The small signal impedance of a three-phase power converter can be expressed in phase ( $abc$ ) domain or sequence domain [7]. And since in three-wire systems, there is no neutral wire, therefore no zero-sequence current can be flowing. Therefore, the zero sequence components and impedances can be neglected. In this paper, the impedances are modelled in the sequence domain because it leads to 2x2 (positive and negative quantities) matrices instead of 3x3 ones ( $abc$  quantities) and also the positive- and negative-sequence impedances of power system components are readily available.

It has been mentioned in [9], that the negative sequence impedance is indeed the complex conjugate of the corresponding positive sequence quantity with the negated frequency.

$$Z_{neg}(j\omega) = (Z_{pos}(-j\omega))^* \quad (1)$$

Therefore, hereafter the positive frequencies are used for positive sequence components and negative frequencies stand for negative sequence.

Fig. 1 shows the considered power converter and how it is connected to the grid, where an  $L$  filter is used. However, this method is also applicable for converters with  $LCL$  filters by changing the grid/converter impedance. It has been shown in [7], [15] that if the effects of the PLL is not neglected then in response to a positive sequence voltage at the PCC, the converter current will have a positive sequence current with the same frequency and a negative sequence current with a different frequency and vice versa. Fig. 2 shows that if the system is balanced, then no other frequencies than the stated ones will appear. The numbers are used to highlight the path that a voltage/current traverses. A voltage perturbation at the grid propagates to the PCC voltage (Block 1 to Block 2), then the power converter in response to this perturbation at the

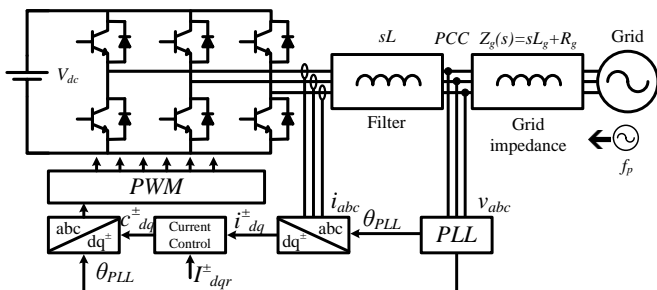


Fig. 1. A current controlled three-phase voltage-source converter.

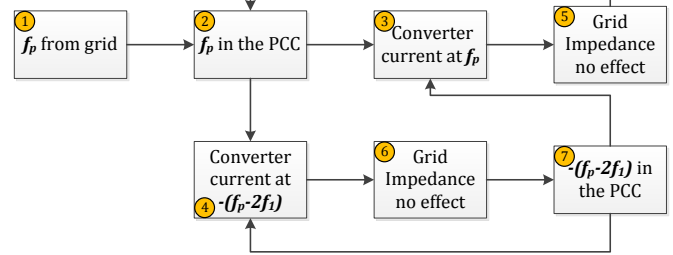


Fig. 2. Perturbation propagation in a balanced power system.

PCC voltage responds with two components, one at  $f_p$  (Block 2 to Block 3) and another one at  $-(f_p - 2f_1)$  (Block 2 to Block 4), where  $f_p$  is the perturbation frequency and  $f_1$  is the fundamental frequency [7], [8]. Since the grid impedance is passive and balanced; the current flow with those frequency components only creates the same frequency and sequence components at the PCC voltage (Block 3 to Block 5 and Block 4 to Block 6). In other words balanced impedance in the sequence domain is decoupled and a current in a sequence cannot induce a voltage at the other sequence. Consequently, the power converter observes a voltage with a frequency of  $-(f_p - 2f_1)$  at the PCC, therefore, the current response would again have two components, one at the same frequency (Block 7 to Block 4) and the other one at  $-(-(f_p - 2f_1) - 2f_1) = f_p$  (Block 7 to Block 3). Thus, the response to the new components in the PCC voltage does not create any new frequencies in the current, and therefore, the loop is closed and one can calculate the closed loop impedance using this.

However, if the grid impedance is unbalanced, in response to a positive sequence current, in addition to a positive sequence voltage it also creates some voltage in the negative sequence. It does not change the frequency; it only injects both sequences to the PCC voltage. The equation for an unbalanced branch, which is shown in Fig. 3, is

$$Z_{\pm} = \begin{bmatrix} Z_{pp} & Z_{pn} \\ Z_{np} & Z_{nn} \end{bmatrix} \quad (2)$$

$$Z_{pp} = Z_{nn} = \frac{1}{3}(Z_1 + Z_2 + Z_3) \quad (3)$$

$$Z_{pn} = (Z_{np})^* = \frac{1}{6}(2Z_1 - Z_2 - Z_3 - j\sqrt{3}(Z_2 - Z_3)) \quad (4)$$

where,  $Z_i$  is the impedance of the  $i^{\text{th}}$  phase and  $Z_{\pm}$  is the impedance matrix in the sequence domain.

As shown in Fig. 4, the imbalance results in an unlimited number of frequency couplings, which makes it difficult to find a closed form equation for the impedances. The converter current has a frequency component at  $-(f_p - 2f_1)$  in response to a voltage perturbation at the PCC. Since, the grid

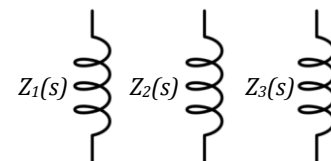


Fig. 3. A three-phase inductive branch.

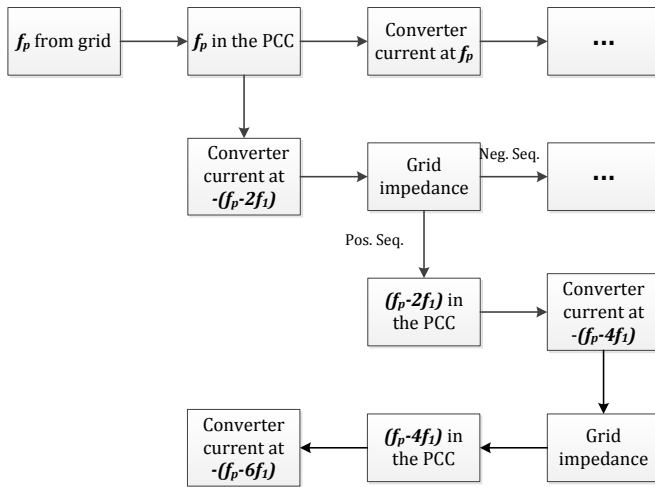


Fig. 4. Perturbation propagation in an unbalanced power system.

impedance is unbalanced, it also creates a reverse sequence voltage drop and therefore, the PCC will have a component at  $(f_p - 2f_1)$ . The converter in response to this new frequency generates a current at  $-(f_p - 4f_1)$ . This cycle never stops and more frequency couplings appear. One can suggest some assumptions for instance, only consider one coupling. However, it might not always be true and in the end the error might not be acceptable [9]. If a matrix-based solution is used, it can consider and calculate all these couplings without any assumptions or simplifications.

### III. THE MATRIX-BASED METHOD

The matrix-based method was first introduced in [13]. It uses the matrix frequency response for all active and passive components, which can be filled in using the theoretical equations (for the components whose transfer functions are known), the simulation or the experimental data, as shown in (5). Each column is the frequency spectrum of the response to a sinusoidal excitation, whose frequency is corresponding to that column.

$$\mathcal{H} = \begin{matrix} \text{Response} \\ \omega_1 \\ \omega_2 \\ \vdots \\ \omega_n \end{matrix} \begin{bmatrix} H_{11}(j\omega_1) & H_{12}(j\omega_2) & \cdots & H_{1n}(j\omega_n) \\ H_{21}(j\omega_1) & H_{22}(j\omega_2) & \cdots & H_{2n}(j\omega_n) \\ \vdots & \vdots & \ddots & \vdots \\ H_{n1}(j\omega_1) & H_{n2}(j\omega_2) & \cdots & H_{nn}(j\omega_n) \end{bmatrix} \begin{matrix} \omega_1 \\ \omega_2 \\ \cdots \\ \omega_n \end{matrix} \quad (5)$$

Excitation

where  $H_{ij}$  is the frequency component of the response at  $\omega = \omega_i$  to a sinusoidal excitation with a frequency at  $\omega = \omega_j$ . It must be noted that these frequencies are necessarily not multiples of the fundamental frequency and in (5)  $\omega_i$  is not the fundamental frequency. For a Linear Time-Invariant (LTI) system there exists only one response at the same frequency of the excitation, therefore, the matrix frequency response will be a diagonal matrix.

The matrix-based method can be considered as the numerical form of the Harmonic Transfer Functions (HTF) for Linear Time Periodic (LTP) systems [16], [17], where the operating point varies periodically. This is the case in AC

systems where all steady state quantities are periodic with the system frequency. One way to study these systems is to use Harmonic State Space (HSS) equations that need complete model of the system under study [18]. However, in this paper it is considered that no information about the structure is available and only the input/output characteristics can be obtained from measurements. The input-output relation of an LTP system in the frequency domain can be described as

$$\mathcal{Y}(s) = \mathcal{H}(s)\mathcal{U}(s) \quad (6)$$

where  $\mathcal{H}(s)$  is the HTF of the system,  $\mathcal{U}(s)$  and  $\mathcal{Y}(s)$  are vectors of frequencies in the input and the output, respectively as follows.

$$\mathcal{Y}(s) = \begin{bmatrix} \vdots \\ Y(s - j\omega_1) \\ Y(s) \\ Y(s + j\omega_1) \\ \vdots \end{bmatrix} \quad (7)$$

$$\mathcal{U}(s) = \begin{bmatrix} \vdots \\ U(s - j\omega_1) \\ U(s) \\ U(s + j\omega_1) \\ \vdots \end{bmatrix} \quad (8)$$

$$\mathcal{H}(s) = \begin{bmatrix} \ddots & \ddots & \ddots & \ddots \\ \ddots & H_0(s - j\omega_1) & H_{-1}(s) & H_{-2}(s + j\omega_1) & \ddots \\ \ddots & H_1(s - j\omega_1) & H_0(s) & H_{-1}(s + j\omega_1) & \ddots \\ \ddots & H_2(s - j\omega_1) & H_1(s) & H_0(s + j\omega_1) & \ddots \\ \ddots & \ddots & \ddots & \ddots & \ddots \end{bmatrix} \quad (9)$$

where,  $\omega_i$  is the angular frequency of the system, and  $H_m(s - jn\omega_1)$  shows the coupling between the input  $U(s - jn\omega_1)$  and the output  $Y(s - j[n-m]\omega_1)$ [16]. Finding the closed form equations for  $H_i(s)$  is very difficult, but by using the small signal perturbations at different frequencies the elements can be filled in numerically. If the HTF of the open loop gain of an LTP system is  $\mathcal{G}(s)$ , then the Generalized Nyquist Criterion (GNC), which is the plot of the eigenvalues of the numerical HTF by sweeping the frequency  $s = j\omega$  in the interval  $(-j\omega_1/2, +j\omega_1/2)$ , can be used to assess the stability of the closed loop system [19].

It can be seen from (9) that for each frequency  $s = j\omega$  a different matrix must be calculated. Infinite number of harmonics cannot be considered and the system must be truncated up to a certain harmonic  $M$ . Instead of calculating the eigenvalues of matrices  $\mathcal{G}(s = -j\frac{\omega_1}{2}) \dots \mathcal{G}(s = +j\frac{\omega_1}{2})$  separately, one can calculate the eigenvalues of  $\mathbb{G}$  as shown in (10), since the eigenvalues of a block-diagonal matrix is the collection of eigenvalues of each sub-matrix.

$$\mathbb{G} = \begin{bmatrix} \left[ \mathcal{G}\left(-j\frac{\omega_1}{2}\right) \right] & 0 & \cdots & 0 \\ 0 & \left[ \mathcal{G}\left(-j\frac{\omega_1}{2} + j\delta\omega\right) \right] & \ddots & \vdots \\ \vdots & \ddots & \ddots & 0 \\ 0 & \cdots & 0 & \left[ \mathcal{G}\left(+j\frac{\omega_1}{2}\right) \right] \end{bmatrix} \quad (10)$$

where,

$$[\mathcal{G}(s)] = \begin{bmatrix} G_0\left(s - j\frac{M}{2}\omega_1\right) & & & & \\ & \ddots & G_{-1}(s) & \ddots & \\ & & G_0(s) & \ddots & \\ & & & G_1(s) & \ddots \\ & & & & G_0\left(s + j\frac{M}{2}\omega_1\right) \end{bmatrix} \quad (11)$$

and  $\delta\omega$  is the frequency resolution of the GNC plot. The frequencies considered in  $\mathcal{G}(s)$  are  $[s - jM\omega_1/2, s - jM\omega_1/2 + j\omega_1, \dots, s + j\omega_1 M/2]$ . If one sorts the rows of  $\mathcal{G}$  based on the frequencies and then sorts the columns, (5) will be obtained. It must be noted that swapping the rows  $i, j$  of a matrix followed by swapping the columns  $i, j$  does not change the eigenvalues. Therefore, (5) can be used for stability studies in a simpler manner compared to (7)-(10). In the authors' view, (5) can be understood easier than (7)-(10) and also the results can be visualized in a better way.

Fig. 5 shows an example of the impedance matrix of a balanced and an unbalanced inductive branch. The horizontal axis is the excitation frequency, the vertical axis is the response frequency and the color intensity of each pixel (square) shows the response magnitude. For instance, most parts of Fig. 5 are white which means the coupling is zero. It must be noted that the dashed lines are only for annotation. As mentioned before, the negative frequency is to model the negative sequence component. It must be noted that the admittance matrix is a complex matrix. However, for the sake of simplicity; only the magnitude is shown here. It can clearly be seen that there are some couplings between the positive- and negative-sequence admittances. For instance, for the balanced case, in response to a +250 Hz perturbation (the red dashed line), there is only one response at +250 Hz (the blue dashed line). However, for the unbalanced case, in addition to the 250 Hz response (response 1: blue dashed line); there is also another component at -250 Hz (response 2: green dashed line), which is weaker than the direct component.

In this paper the imbalance is in focus, and therefore, an unbalanced current controller must be utilized to successfully track the references, otherwise the controller fails due to the adverse effect of negative sequence component in a dq transformation [20]. In order to handle both positive and negative sequences a Sequence Extraction Block (SEB) must be used that extracts the positive and negative sequence components in the  $dq$  signals correctly. The highlighted block in Fig. 6 is the block diagram of a SEB based on the Decoupled Double Synchronous Reference Frame (DDSRF) that has first been described in [20].  $T_{dq}$  is the Park's transformation and

$$F = \frac{\omega_f}{s + \omega_f} \quad (12)$$

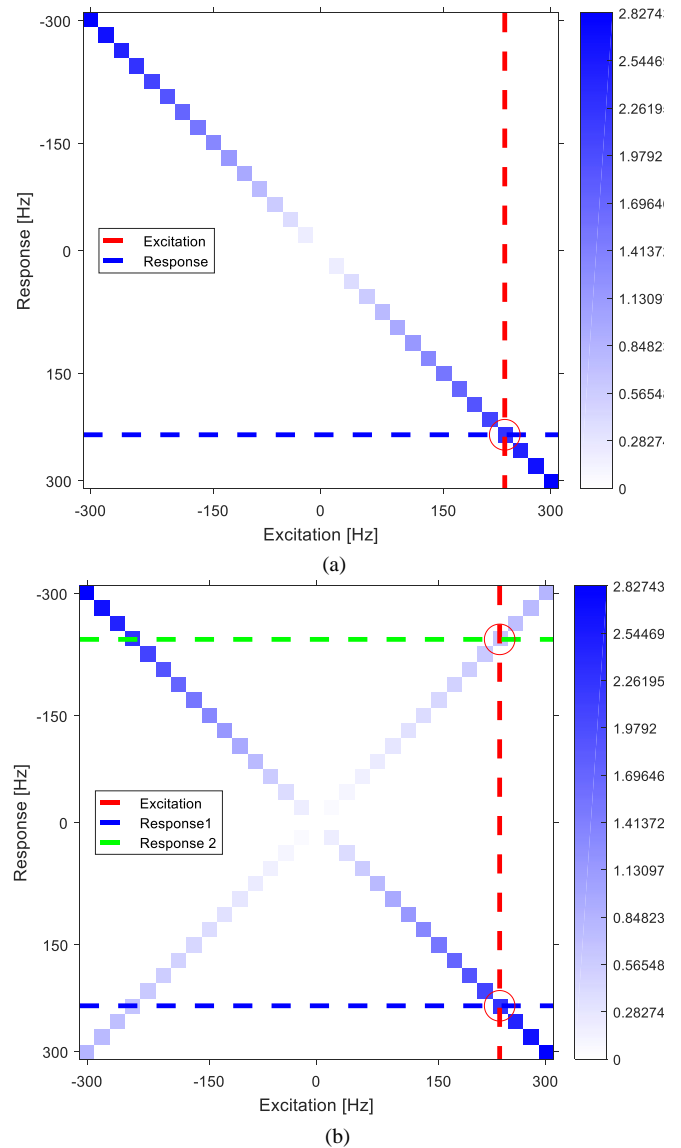


Fig. 5. The impedance matrix of an inductive branch as shown in Fig. 3 (a) a balanced case. (b) an unbalanced case.

$$T_{dq^2}(\theta) = \begin{bmatrix} \cos(2\theta) & \sin(2\theta) \\ -\sin(2\theta) & \cos(2\theta) \end{bmatrix} \quad (13)$$

where  $\theta$  is the phase angle of the PLL and  $\omega_f = \omega_1/\sqrt{2}$  in order to have a good performance [21].

As it is shown in Fig. 6, the SEB needs the phase

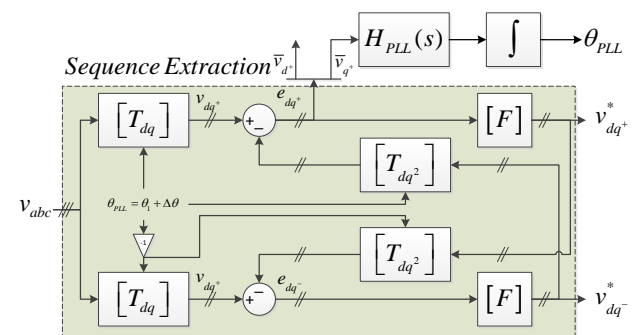


Fig. 6. A DDSRF PLL, where the highlighted area is the Sequence Extraction Block [21].

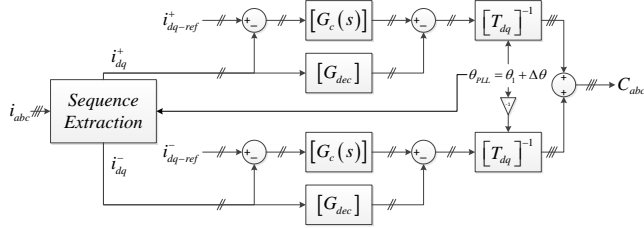


Fig. 7. A Decoupled Double Synchronous Reference Frame current controller [22], [23].

information of the positive sequence voltage. This can be done by using a simple Synchronous Reference Frame (SRF) PLL to synchronize to the positive sequence voltage as shown in Fig. 6.

In this paper the current controller also utilizes the same SEB to regulate the positive-/negative-sequence currents. Fig. 7 shows a block diagram of this controller [22], [23], where the current controller blocks are

$$[G_c(s)] = \begin{bmatrix} H_i(s) & 0 \\ 0 & H_i(s) \end{bmatrix} \quad (14)$$

$$[G_{dec}] = \begin{bmatrix} 0 & K_d \\ -K_d & 0 \end{bmatrix} \quad (15)$$

and  $H_i(s)$  is a PI controller and  $G_{dec}$  minimizes the couplings between the dq signals.

In this paper the admittance matrix of a power converter, whose parameters are listed in Table I and Table III (stable case), is filled in using simulations and no equation is used for stability analysis. At each simulation, a small signal perturbation in the voltage with a defined frequency is directly applied to the converter terminals without any grid impedance. The admittance by definition is the changes in the current due to a change in the terminal voltage. Therefore, for each excitation frequency a column of (5) is filled in based on the FFT of the current. However, the linearized models, which are used, are dependent on the operating point, and if the operating point (i.e. the output current and the PCC voltage) is changed (which is a valid assumption in a wind farm), then the whole identification process must be repeated. In [13] it has been shown that the linearized admittance matrix of a power converter changes linearly with the operating point (i.e. the output current and the PCC voltage). Therefore, by calculating these linear characteristics once, the admittance can be calculated at any conditions. The considered system in [13] is a balanced system, and one may question the linearity

TABLE I. PARAMETERS OF THE GRID-CONNECTED INVERTER FOR SIMULATION

Symbol	Description	Value
$f_l$	Grid frequency	50 Hz
$L$	Filter inductance	1.5 mH
$R$	Filter equivalent resistance	0.5 $\Omega$
$V_{dc}$	Inverter dc voltage	600 V
$K_p$	Proportional gain of the current controller	0.01
$K_i$	Integrator gain of current controller	0.1
$BW_{PLL}$	Bandwidth of PLL	65 Hz
$K_d$	Decoupling term	0

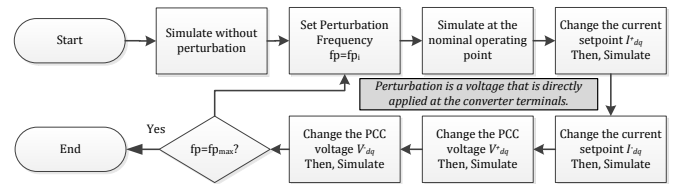


Fig. 9. How to calculate the parameters that are needed for the matrix-based method.

TABLE II. COMPARING THE PREDICTED RESULTS WITH THE SIMULATIONS

Frequency	110 Hz		10 Hz	
	Theory	Sim.	Theory	Sim.
$ I_a $	0.0240	0.0244	0.1600	0.1614
$\angle I_a$	0.053	0.032	0.142	0.180
$ I_b $	0.0282	0.0286	0.1534	0.1557
$\angle I_b$	-2.373	-2.407	2.336	2.369
$ I_c $	0.0187	0.0187	0.1431	0.1455
$\angle I_c$	1.771	1.738	-1.9433	-1.902

assumption here because the system under study is now unbalanced. Hence, the operating point quantities, voltage and current at PCC (for both sequences) are changed (the perturbation frequency is fixed at 110 Hz) to see whether the relationship is linear or not. Fig. 8 indicates that all electrical quantities behave linearly except for the positive sequence voltage (note absolute value is plotted). This is due to the PLL that uses the positive sequence voltage and is a nonlinear block in the low frequency range. However, Fig. 8 (c) reveals that if the PCC voltage lies in the interval (0.95, 1.05) p.u. then it can be considered as a linear function. This is a valid assumption in power systems, where the voltages are kept inside this interval by reactive power control. In a wind farm, wind turbines can also support the PCC voltage by injecting or absorbing the reactive power. Thus, one can use (16) to calculate the admittance matrix at any other conditions, if the partial derivatives, which describe the linear characteristics, are available.

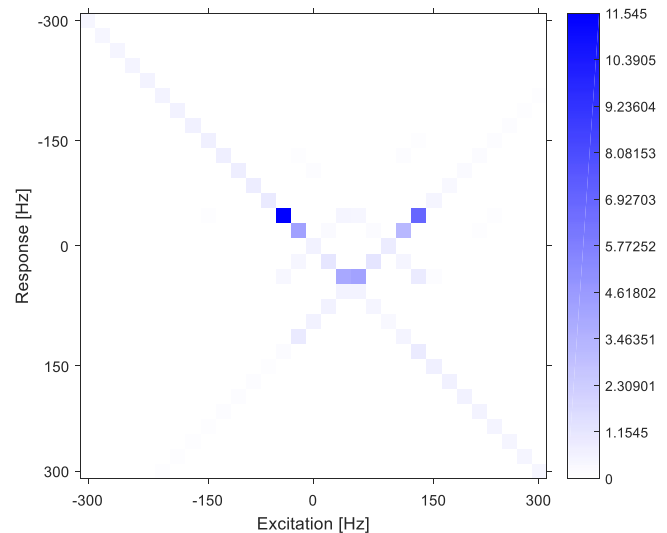


Fig. 10. A Decoupled Double Synchronous Reference Frame current controller [22], [23].

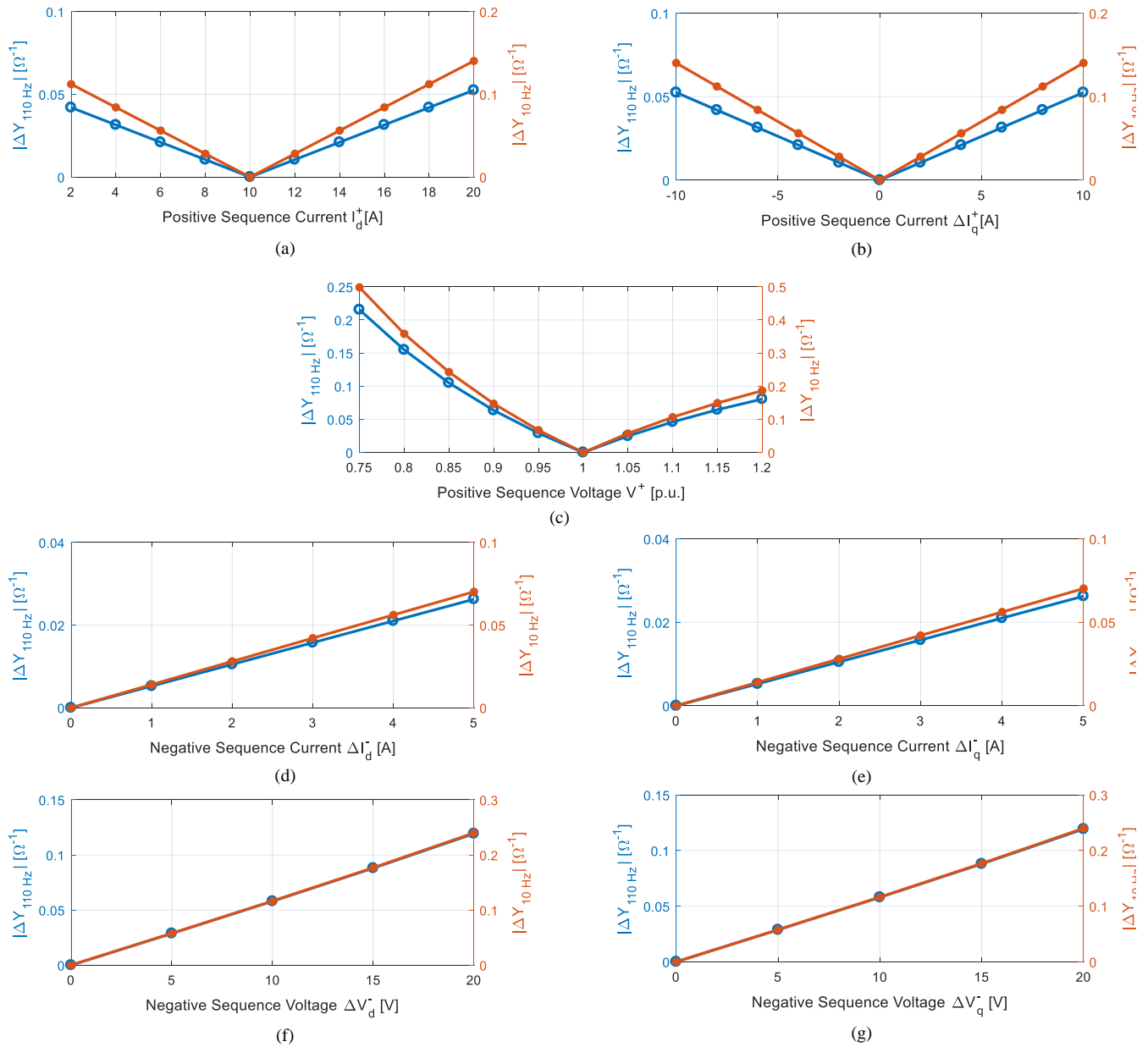


Fig. 8. The admittance change versus: (a) the positive sequence current reference d channel  $I_d^+$ . (b) the positive sequence current reference q channel  $I_q^+$ . (c) the positive sequence voltage at the PCC. (d) the negative sequence current reference d channel  $I_d^-$ . (e) the negative sequence current reference q channel  $I_q^-$ . (f) the negative sequence voltage at the PCC d channel  $V_d^-$ . (g) the negative sequence voltage at the PCC q channel  $V_q^-$ .

$$\begin{aligned}
 & Y(V_{dq}^+ + \Delta V_{dq}^+, I_{dq}^+ + \Delta I_{dq}^+, V_{dq}^-, I_{dq}^- + \Delta I_{dq}^-) \\
 & \approx Y(V_{dq}^+, I_{dq}^+, V_{dq}^-, I_{dq}^-) + \frac{\partial Y}{\partial V_{dq}^+} \Delta V_{dq}^+ + \frac{\partial Y}{\partial I_{dq}^+} \Delta I_{dq}^+ \\
 & \quad + \frac{\partial Y}{\partial V_{dq}^-} \Delta V_{dq}^- + \frac{\partial Y}{\partial I_{dq}^-} \Delta I_{dq}^-
 \end{aligned} \quad (16)$$

The partial derivatives in (16) can easily be found by the procedure illustrated in Fig. 9. For instance, by repeating the simulation for another positive-sequence current set point while all other quantities (PCC voltage both positive and negative components, current control parameters and etc.) are kept constant, the rate of the change in the admittance to a change in the injected positive sequence current  $\frac{\partial Y}{\partial I_{dq}^+}$  can be

found.

To verify (16), the converter admittance at a new and untrained operating point ( $v_{dq}^+=95$ ,  $I_{dq}^+=20+j5$ ,  $V_{dq}^-=10+j5$ ,  $I_{dq}^-=2+j2$ ,  $f_p=110$  Hz) is anticipated using (16) and is verified by time domain simulations as shown in Table II. Fig. 10 shows the admittance matrix of the power converter.

#### IV. SIMULATION RESULTS

The operating point of the converter depends on the network configuration and the voltages and currents in the network. Therefore, the first step is to run a load flow and calculate the operating point. At this stage the converter can be modelled as a constant power element. Then, the load flow data are used as the initial points and the linearized matrix of the converter can be found using (16).

To show the effectiveness of the method, two studies will be presented. The first case is used for stability evaluation of the system, while the other one is used for power quality studies in the system. In both cases the system shown in Fig. 1 is used, where the current controller and the PLL are based on Fig. 7 and Fig. 6, respectively.

### A. Case 1: Stability of an unbalanced system

In this part, the considered converter is connected to an unbalanced grid, where the imbalance is intentionally set too large to do some comparisons (see Table III). The controller regulates the positive sequence current and keeps the negative sequence current to zero. Therefore, the objective is to inject balanced current that is synchronized with the positive sequence voltage at the PCC. All elements are modelled as matrix impedances/admittances. The method is used to evaluate the stability based on the matrix form of the impedance based stability criterion [13], where the eigenvalues of the minor loop gain in the matrix form (the product of the grid impedance and the converter admittance, both are matrices) are plotted.

It can be seen from Fig. 11 that when the output current set point is lowered from 20 A to 2 A, the system becomes unstable. This conclusion is also verified by time domain

TABLE III. THE PARAMETERS OF THE GRID

Symbol	Description	Value
$V_g^+$	Grid line-ground peak voltage (Pos. Seq.)	100 V
$I_{dr}^+$	Pos. seq. d channel current reference (stabe/unstable cases)	20/2 A
$I_{qr}^+$	Pos. seq. q channel current reference	0 A
$I_{dr}^-$	Neg. seq. d channel current reference	0 A
$I_{qr}^-$	Neg. seq. q channel current reference	0 A
$L_1$	Grid inductance-phase A (unbalanced/balanced)	2.3 / 2.3 mH
$L_2$	Grid inductance-phase B (unbalanced/balanced)	1.1 / 2.3 mH
$L_3$	Grid inductance-phase C (unbalanced/balanced)	3.4 / 2.3 mH

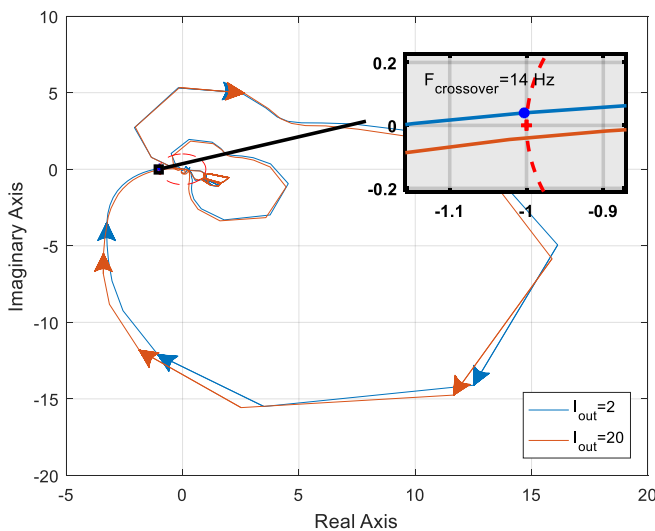


Fig. 11. The generalized Nyquist plot of the unbalanced system when the output current is changed.

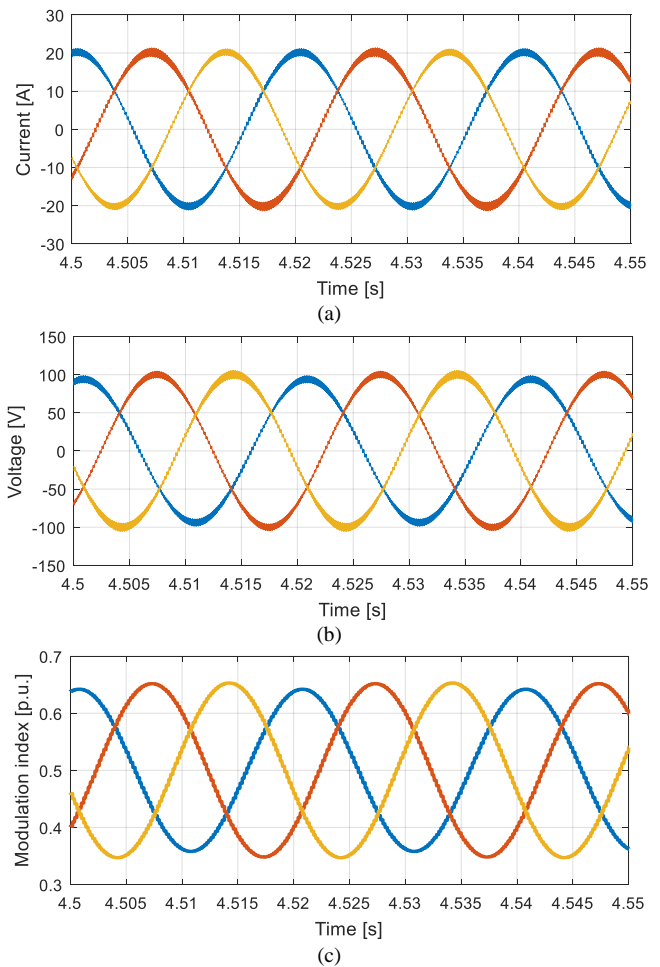


Fig. 12. Time domain simulations of the unbalanced system, when the output current set point is 20 A (a) the output current (b) the PCC voltage (c) the modulation indices.

simulations of a full detailed model as shown in Fig. 12 and Fig. 13. The PCC voltage as shown in Fig. 12 (b) and Fig. 13 (b) is around the nominal value; therefore, there is no problem with the nonlinearity of the PCC voltage as described by Fig. 8 (c). Fig. 13 shows that the converter is unable to regulate the output current due to the instability. One may ask that if the system is unstable why the converter is not saturated as shown in Fig. 13 (c), the modulation indices are below 100%. The current system is a nonlinear system and small signal linearization is used to find a linear model. Therefore, all conclusions are valid for a small signal region around the operating point. In large signal, sometimes a nonlinear system is attracted to a limit cycle [24], [25] and does not necessarily go to infinity. However, the results of the small signal studies are valuable; because they can clearly state that the behavior is not as expected in a given operating point (uncontrolled currents and harmonics). The frequency spectrum of the output current and the PCC voltage indicates that the frequency of instability is around 14 Hz. This frequency can also be predicted by looking at the crossover frequency (intersection with the unity circle) of the Nyquist plot shown in Fig. 11.



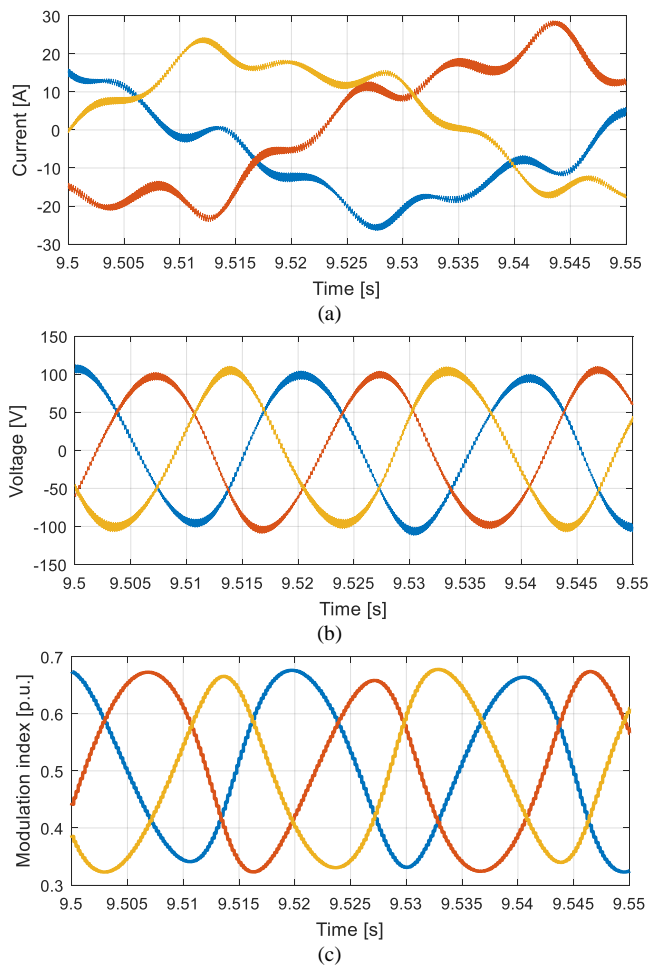


Fig. 13. Time domain simulations for the unbalanced system, when the output current set point is 2 A (a) the output current (b) the PCC voltage (c) the modulation indices.

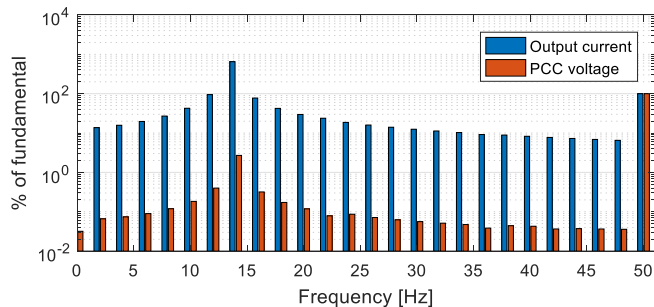


Fig. 14. The frequency spectrum of the output current and the PCC voltage, when the output current setpoint is 2 A (the unstable case).

To see what is exactly the effect of imbalance, the previous case is now repeated with a balanced grid, where the inductance values are the average of the unbalanced inductances. Based on (4), by using the average values, the positive/negative sequence impedance are not changed. It can be seen from Fig. 15, Fig. 16 and Fig. 17 that the Nyquist plots and the time domain results are closely correlated. In other words, that large changes in the grid did not influence the results so much, and one can say that the balanced case is even worse than the unbalanced case (the Nyquist plot is closer to the critical point), and therefore, if the balanced case is only studied it gives a more conservative result in this case.

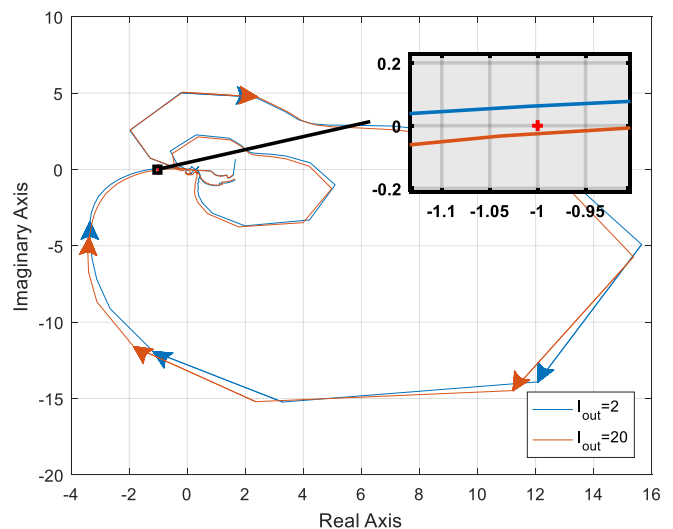


Fig. 15. The generalized Nyquist plot of the unbalanced system when the output current is changed.

### A. Case 2: The power quality studies

By knowing the harmonic sources and matrix impedances, the harmonics at different points can be found using some simple electrical network equations. For instance, for the simple case that is presented in Fig. 1, if the harmonics content

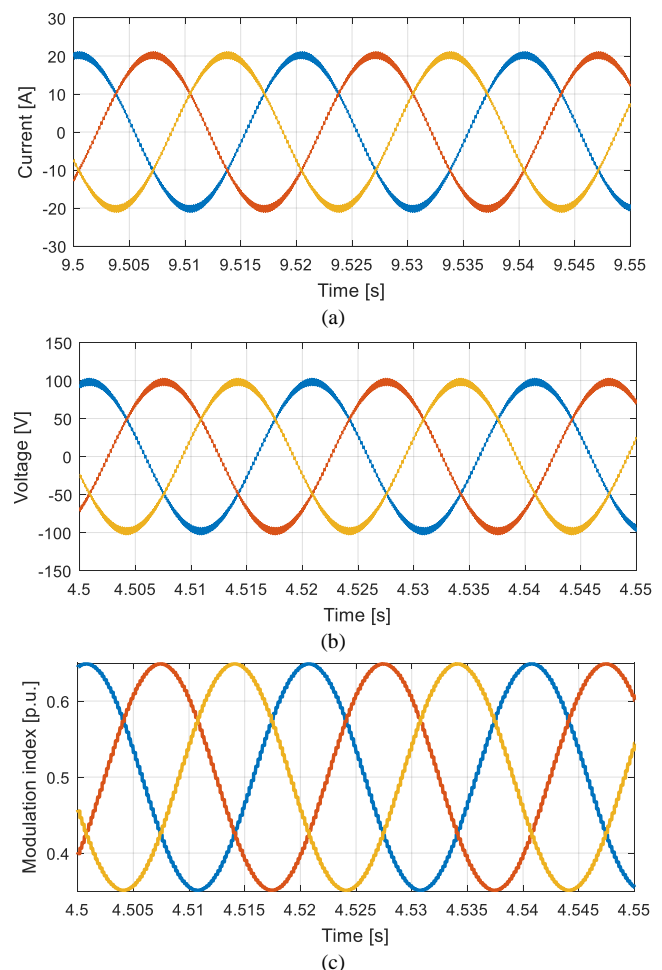


Fig. 16. Time domain simulations for the balanced system, when the output current set point is 20 A (a) the output current (b) the PCC voltage (c) the modulation indices.

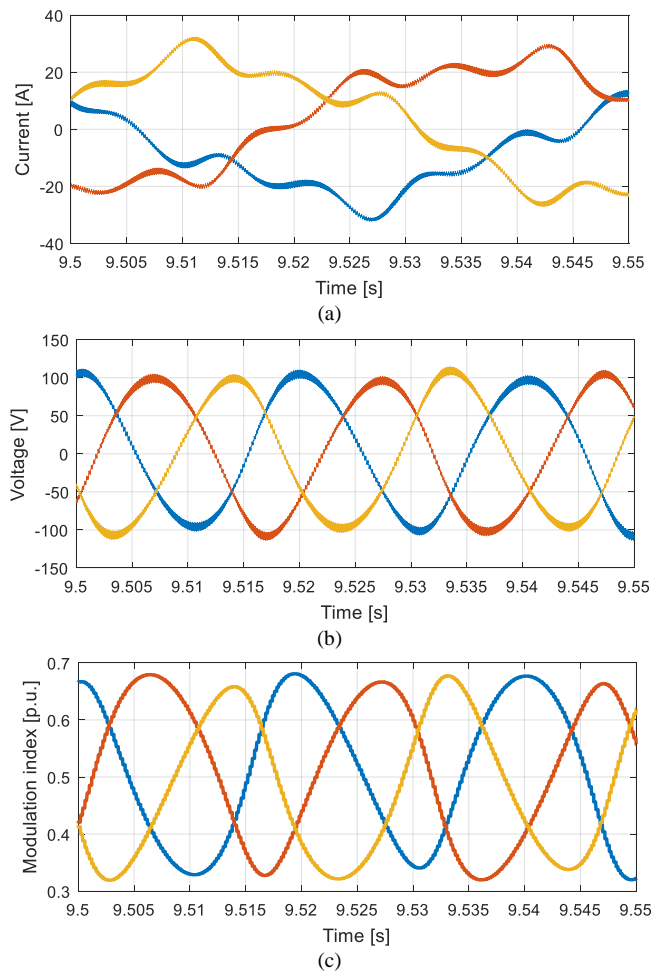


Fig. 17. Time domain simulations for the balanced system, when the output current set point is 2 A (a) the output current (b) the PCC voltage (c) the modulation indices.

in the grid is known (as a vector that contains all frequencies), then the harmonics at the PCC can easily be found using (17).

$$[V_{PCC}] = [Z_c][Z_g + Z_c]^{-1}[V_g] \quad (17)$$

where,  $[Z_c]$  is the impedance matrix of the converter (inverse of the admittance matrix),  $[Z_g]$  is the impedance matrix of the grid and  $[V_g]$  is the present harmonics at the grid.

The phasor plot shown in Fig. 18 is for the previous case, where the system is unbalanced but all the current set points are now non-zero as stated in Table IV. To show the effectiveness of the proposed method, it is assumed that the grid has a positive sequence inter-harmonic component at 90 Hz. It can be seen that due to the aforementioned couplings at the PCC, an additional 10 Hz ( $-(f_p - 2f_l)$ ) component can also be seen, which surprisingly is even larger than the 90 Hz component for the currents. It can be seen that the results from theoretical equations using the matrix-based method are in good agreement with the results of the time domain simulations. Fig. 19 show the time domain results of this case, where the effects of the 10 Hz components is significant in the output current.

## V. CONCLUSION

In this paper, a numerical matrix-based method for

TABLE IV. THE CURRENT SET POINTS FOR THE SECOND CASE STUDY

Symbol	Description	Value
$I_{dr}^+$	Pos. seq. d channel current reference (stable/unstable cases)	20 A
$I_{qr}^+$	Pos. seq. q channel current reference	5 A
$I_{dr}^-$	Neg. seq. d channel current reference	2 A
$I_{qr}^-$	Neg. seq. q channel current reference	2 A

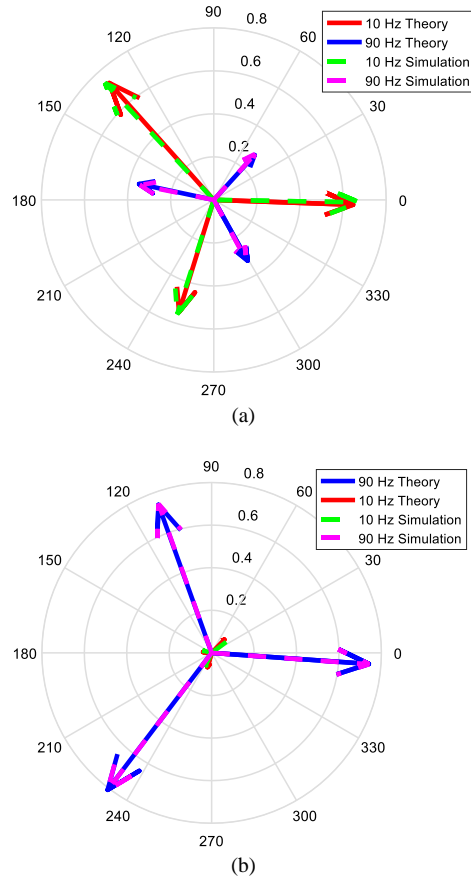


Fig. 18. The phasor plot of (a) harmonic currents and (b) harmonic voltages at the PCC found by theory and simulations.

harmonic studies in unbalanced networks is proposed. The method is able to deal with the couplings between the positive and negative sequence impedances due to the outer loop controls and also the asymmetrical transmission assets. The method is proved by the HTF concept in studying LTP systems. The admittance matrix of the converter is a nonlinear function of the positive sequence voltage of the PCC but is a linear function of the output current. If the PCC voltage is kept close to the nominal value, then, no matter how much the current is changed, the admittance can be calculated. This is also the case in a wind farm where the output power (current) is changing a lot depending on the wind speed and voltage magnitudes are almost constant. The proposed method is verified by time domain simulation of a full detailed model and it is shown that based on the results of this study some simplifications can be made. For instance, it seems that if the system is well designed for a balanced case (i.e. enough stability margins), the stability is even better in the unbalanced case. However, proving this needs a more detailed discussion with analytical formulation, which is not the subject of this paper. The proposed method can also be used for power

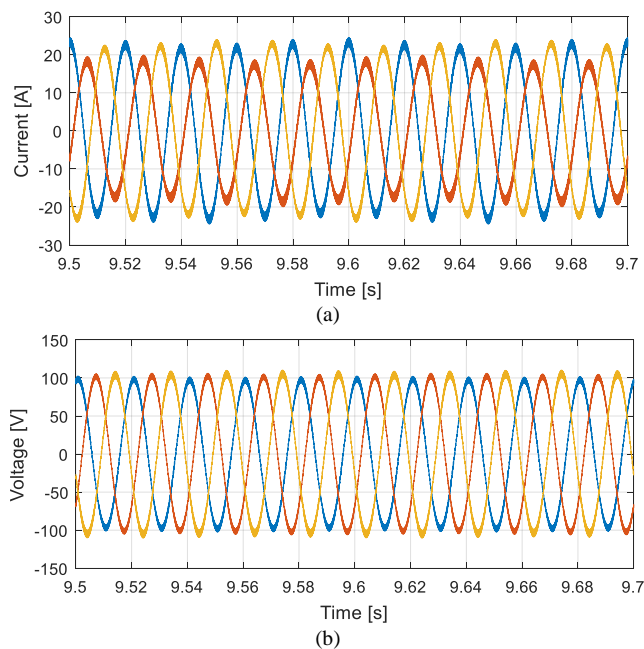


Fig. 19. Time domain results of (a) the output current and (b) the PCC voltage, when the grid has an interharmonic at 90 Hz.

quality studies to include the effects of coupling. It is shown that in the low frequency range, the couplings should not be neglected due to the fact that their effect might be even larger.

#### REFERENCES

[1] P. Brogan, "The stability of multiple, high power, active front end voltage sourced converters when connected to wind farm collector systems," in *EPE Wind Energy Chapter Seminar*, pp. 1–6, 2010.

[2] Ł. Kocewiak, S. Chaudhary, and B. Hesselbæk, "Harmonic Mitigation Methods in Large Offshore Wind Power Plants," in *The 12th International Workshop on Large-Scale Integration of Wind Power into Power Systems as well as Transmission Networks for Offshore Wind Farms*, 2013, pp. 443–448.

[3] Ł. H. Kocewiak, J. Hjerrild, and C. L. Bak, "Wind turbine converter control interaction with complex wind farm systems," *IET Renew. Power Gener.*, vol. 7, no. 4, pp. 380–389, Jul. 2013.

[4] Z. Shuai, D. Liu, J. Shen, C. Tu, Y. Cheng, and A. Luo, "Series and Parallel Resonance Problem of Wideband Frequency Harmonic and Its Elimination Strategy," *IEEE Trans. Power Electron.*, vol. 29, no. 4, pp. 1941–1952, Apr. 2014.

[5] J. Sun, "Impedance-based stability criterion for grid-connected inverters," *IEEE Trans. Power Electron.*, vol. 26, no. 11, pp. 3075–3078, 2011.

[6] X. Wang, F. Blaabjerg, and W. Wu, "Modeling and Analysis of Harmonic Stability in an AC Power-Electronics-Based Power System," *IEEE Trans. Power Electron.*, vol. 29, no. 12, pp. 6421–6432, 2014.

[7] M. K. Bakhshizadeh, X. Wang, F. Blaabjerg, J. Hjerrild, L. Kocewiak, C. L. Bak, and B. Hesselbæk, "Couplings in Phase Domain Impedance Modelling of Grid-Connected Converters," *IEEE Trans. Power Electron.*, vol. 31, no. 10, pp. 6792–6796, 2016.

[8] A. Rygg, M. Molinas, Z. Chen, and X. Cai, "A modified sequence domain impedance definition and its equivalence to the dq-domain impedance definition for the stability analysis of AC power electronic systems," *IEEE J. Emerg. Sel. Top. Power Electron.*, vol. 4, no. 4, pp. 1383–1396, 2016.

[9] M. K. Bakhshizadeh, J. Hjerrild, L. Kocewiak, B. Hesselbæk, X. Wang, F. Blaabjerg, and C. L. Bak, "Small-signal model of a decoupled double synchronous reference frame current controller," in *2016 IEEE 17th Workshop on Control and Modeling for Power Electronics (COMPEL)*, 2016, pp. 1–6.

[10] C. F. Jensen, Z. Amin, and Ł. Kocewiak, "Amplification of Harmonic

Background Distortion in Wind Power Plants with Long High Voltage Connections," in *CIGRE 2016 Session*, 2016.

[11] B. Wen, D. Boroyevich, R. Burgos, P. Mattavelli, and Z. Shen, "Analysis of D-Q Small-Signal Impedance of Grid-Tied Inverters," *IEEE Trans. Power Electron.*, vol. 31, no. 1, pp. 675–687, Jan. 2016.

[12] L. Harnefors, "Modeling of three-phase dynamic systems using complex transfer functions and transfer matrices," *IEEE Trans. Ind. Electron.*, vol. 54, no. 4, pp. 2239–2248, Aug. 2007.

[13] M. K. Bakhshizadeh, J. Hjerrild, L. H. Kocewiak, F. Blaabjerg, C. L. Bak, X. Wang, F. M. F. da Silva, and B. Hesselbæk, "A Numerical Matrix-Based method in Harmonic Studies in Wind Power Plants," in *15th Wind Integration Workshop*, 2016, pp. 335–339.

[14] M. K. Bakhshizadeh, F. Blaabjerg, C. Leth Bak, F. Faria da Silva, J. Hjerrild, K. Lukasz, B. Hesselbæk, and T. Sørensen, "Harmonic Modelling, Propagation and Mitigation for Large Wind Power Plants Connected via Long HVAC Cables: Review and Outlook of Current Research," in *IEEE ENERGYCON 2016*, 2016, pp. 1–5.

[15] X. Wang, L. Harnefors, F. Blaabjerg, and P. C. Loh, "A unified impedance model of voltage-source converters with phase-locked loop effect," in *2016 IEEE Energy Conversion Congress and Exposition (ECCE)*, 2016, pp. 1–8.

[16] E. Möllerstedt, "Dynamic analysis of harmonics in electrical systems," Ph.D. dissertation, Department of Automatic Control, Lund Institute of Technology (LTH), 2000.

[17] N. M. Wereley, "Analysis and control of linear periodically time varying systems," Massachusetts Institute of Technology, 1990.

[18] J. B. Kwon, X. Wang, F. Blaabjerg, C. L. Bak, A. R. Wood, and N. R. Watson, "Harmonic Instability Analysis of a Single-Phase Grid-Connected Converter Using a Harmonic State-Space Modeling Method," *IEEE Trans. Ind. Appl.*, vol. 52, no. 5, pp. 4188–4200, 2016.

[19] S. R. Hall and N. M. Wereley, "Generalized Nyquist Stability Criterion for Linear Time Periodic Systems," in *1990 American Control Conference*, 1990, pp. 1518–1525.

[20] P. Rodriguez, J. Pou, J. Bergas, J. I. Candela, R. P. Burgos, and D. Boroyevich, "Decoupled Double Synchronous Reference Frame PLL for Power Converters Control," *IEEE Trans. Power Electron.*, vol. 22, no. 2, pp. 584–592, Mar. 2007.

[21] R. Teodorescu, M. Liserre, and P. Rodríguez, *Grid Converters for Photovoltaic and Wind Power Systems*. IEEE-Wiley, 2011.

[22] M. Reyes, P. Rodriguez, S. Vazquez, A. Luna, R. Teodorescu, and J. M. Carrasco, "Enhanced Decoupled Double Synchronous Reference Frame Current Controller for Unbalanced Grid-Voltage Conditions," *IEEE Trans. Power Electron.*, vol. 27, no. 9, pp. 3934–3943, Sep. 2012.

[23] M. Reyes, P. Rodriguez, S. Vazquez, A. Luna, J. M. Carrasco, and R. Teodorescu, "Decoupled Double Synchronous Reference Frame current controller for unbalanced grid voltage conditions," in *2012 IEEE Energy Conversion Congress and Exposition (ECCE)*, 2012, pp. 4676–4682.

[24] Ł. Kocewiak, C. L. Bak, and S. Munk-Nielsen, "Bifurcation and Chaos in a Pulse Width modulation controlled Buck Converter," in *Proc. of the 6th Eurosim Congress on Modelling and Simulation*, 2007.

[25] P. Blanchard, R. L. Devaney, and G. R. Hall, *Differential equations*. Thomson Brooks/Cole, 2006.



**Mohammad Kazem Bakhshizadeh** (S'16) received the B.S. and M.S. degrees in electrical engineering from the Amirkabir University of Technology, Tehran, Iran in 2008 and 2011, respectively. He is currently an industrial PhD student at Aalborg University, Aalborg, Denmark in collaboration with DONG Energy Wind Power, Fredericia, Denmark. In 2016, he was a visiting scholar at Imperial College London, London, U.K. His research interests include power quality, modeling and control of power converters, and grid converters for renewable energy systems.



**Frede Blaabjerg** (S'86–M'88–SM'97–F'03) was with ABB-Scandia, Randers, Denmark, from 1987 to 1988. From 1988 to 1992, he got the PhD degree in Electrical Engineering at Aalborg University in 1995. He became an Assistant Professor in 1992, an Associate Professor in 1996, and a Full Professor of

power electronics and drives in 1998. From 2017 he became a Villum Investigator.

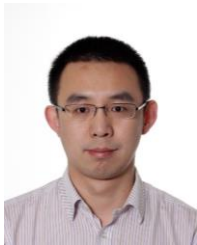
His current research interests include power electronics and its applications such as in wind turbines, PV systems, reliability, harmonics and adjustable speed drives. He has published more than 450 journal papers in the fields of power electronics and its applications. He is the co-author of two monographs and editor of 6 books in power electronics and its applications.

He has received 18 IEEE Prize Paper Awards, the IEEE PELS Distinguished Service Award in 2009, the EPE-PEMC Council Award in 2010, the IEEE William E. Newell Power Electronics Award 2014 and the Villum Kann Rasmussen Research Award 2014. He was the Editor-in-Chief of the IEEE TRANSACTIONS ON POWER ELECTRONICS from 2006 to 2012. He has been Distinguished Lecturer for the IEEE Power Electronics Society from 2005 to 2007 and for the IEEE Industry Applications Society from 2010 to 2011 as well as 2017 to 2018.

He is nominated in 2014, 2015 and 2016 by Thomson Reuters to be between the most 250 cited researchers in Engineering in the world. In 2017 he became Honoris Causa at University Politehnica Timisoara (UPT), Romania.



**Jesper Hjerrild** was born in 1971. He holds an MSc and PhD degrees in electrical engineering from the Technical University of Denmark, Lyngby, in 1999 and 2002, respectively. Currently, he is employed with DONG Energy. His main technical interest is electrical power systems in general, involving a variety of technical disciplines including modeling of power system including wind power and power system control, stability and harmonics. Furthermore, he also works with designing of the wind farm.



**Xiongfei Wang** (S'10–M'13–SM'17) received the B.S. degree from Yanshan University, Qinhuangdao, China, in 2006, the M.S. degree from Harbin Institute of Technology, Harbin, China, in 2008, both in electrical engineering, and the Ph.D. degree in energy technology from Aalborg University, Aalborg, Denmark, in 2013.

Since 2009, he has been with the Aalborg University, Aalborg, Denmark, where he is currently an Associate Professor in the Department of Energy Technology. His research interests include modeling and control of grid-connected converters, harmonics analysis and control, passive and active filters, stability of power electronic based power systems.

Dr. Wang serves as an Associate Editor for the IEEE TRANSACTIONS ON POWER ELECTRONICS, the IEEE TRANSACTIONS ON INDUSTRY APPLICATIONS, and the IEEE JOURNAL OF EMERGING AND SELECTED TOPICS IN POWER ELECTRONICS. He is also the Guest Editor for the Special Issue “Grid-Connected Power Electronics Systems: Stability, Power Quality, and Protection” in the IEEE TRANSACTIONS ON INDUSTRY APPLICATIONS. He received the second prize paper award and the outstanding reviewer award of IEEE TRANSACTIONS ON POWER ELECTRONICS in 2014 and 2017, respectively, and the best paper awards at IEEE PEDG 2016 and IEEE PES GM 2017.



**Claus Leth Bak** was born in Århus, Denmark, on April 13<sup>th</sup>, 1965. He received the B.Sc. with honors in Electrical Power Engineering in 1992 and the M.Sc. in Electrical Power Engineering at the Department of Energy Technology (ET) at Aalborg University (AAU) in 1994. After his studies he worked as a professional engineer with

Electric Power Transmission and Substations with specializations within the area of Power System Protection at the NV Net Transmission Company. In 1999 he was employed as an Assistant Professor at ET-AAU, where he holds a Full Professor position today. He received the PhD degree in 2015 with the thesis “EHV/HV underground cables in the transmission system”. He has supervised/co-supervised +35 PhD's and +50 MSc theses. His main Research areas include Corona Phenomena on Overhead Lines, Power System Modeling and Transient Simulations, Underground Cable transmission, Power System Harmonics, Power System Protection and HVDC-VSC Offshore Transmission Networks. He is the author/coauthor of app. 240 publications. He is a member of Cigré JWG C4-B4.38, Cigré SC C4 and SC B5 study committees' member and Danish Cigré National Committee. He is an IEEE senior member (M'1999, SM'2007). He received the DPSP 2014 best paper award and the PEDG 2016 best paper award. He serves as Head of the Energy Technology PhD program (+ 100 PhD's) and as Head of the Section of Electric Power Systems and High Voltage in AAU and is a member of the PhD board at the Faculty of Engineering and Science.



**Lukasz Hubert Kocewiak** (M'12, SM'16) holds BSc and MSc degrees in electrical engineering from Warsaw University of Technology as well as PhD degree from Aalborg University.

Currently he is with DONG Energy Wind Power and is working as a senior power system engineer on development of electrical infrastructure in large offshore

wind power plants.

The main direction of his research is related to harmonics and nonlinear dynamics in power electronics and power systems especially focused on wind power generation units.

He is the author/co-author of more than 60 publications. He is a member of various working groups within Cigré, IEEE, IEC.